



Supporting Online Material for

Dentate Gyrus NMDA Receptors Mediate Rapid Pattern Separation in the Hippocampal Network

Thomas J. McHugh, Matthew W. Jones, Jennifer J. Quinn, Nina Balthasar, Roberto Coppari, Joel K. Elmquist, Bradford B. Lowell, Michael S. Fanselow, Matthew A. Wilson, Susumu Tonegawa*

*To whom correspondence should be addressed. E-mail: tonegawa@mit.edu

Published 7 June 2007 on *Science Express*
DOI: 10.1126/science.1140263

This PDF file includes:

Materials and Methods
SOM Text
Figs. S1 to S6
Tables S1 to S3
References

Supporting Online Material

1. Materials and Methods

Generation of Animals

The POMC-Cre construct used to generate the mice has been previously described (1). The line used in this study was generated in an identical manner and then was rederived and backcrossed for three generations in the C57BL/6 genetic background prior to use. To fully characterize the pattern of Cre expression the line was crossed with the Rosa26 reporter line (2). For the production of DG-NR1 KO mice the POMC-Cre line was crossed with the "floxed" NMDA receptor subunit-1 (*fNR1*) mouse line (3), which has been maintained in a C57BL/6 background. Males homozygous for the *fNR1* allele and carrying the POMC-Cre transgene were then crossed to homozygous *fNR1* females from the colony to produce all subsequent DG-NR1 KO and *fNR1* littermate control mice. Tail DNA from all offspring was genotyped for the presence of Cre (5' primer agatgttcgcgattatc; 3' Primer agctacaccagagacgg; Cycle: 2'@94°; 10''@94°, 1'@55°, 1'@72° x35; 5'@72°C), as well as for the presence of a recombined NR1 allele (5' primer agt tccacaccagccagagc; 3' Primer aggggaggagtagaaggtgg; Cycle: 2'@94°; 10''@94°, 1'30''@69° x35; 5'@72°C) in the germline, an event that occurs at a low frequency. All procedures relating to animal care and treatment conformed to the Institutional and NIH guidelines.

Histology and Immunohistochemistry

Mice were transcardially perfused with 4% paraformaldehyde (PFA) in 0.1 M sodium phosphate buffer (PB). For X-Gal staining the brains were then removed and post fixed for 30 minutes in 4% PFA. Coronal sections (50 µm thick) were cut on a Vibratome and collected in PB. Sections were first incubated in 0.1 M PB containing 0.01% SDS, 0.02% NP-40, 2 mM MgCl₂ at 4°C for 15 minutes, followed by the β-galactosidase reaction in 1xPBS pH 8.0 containing 0.5 mg/ml X-gal, 5 mM K₄Fe(CN)₆•3H₂O, 5 mM K₃Fe(CN)₆, 2 mM MgCl₂ at 37°C for 24 hours. Section were

post fixed in 10% formalin for at least 2 hours, and counterstained with Nuclear Fast Red. For the immunofluorescent staining in figures 1B to 1H brains were post fixed in 4% PFA and 50 μ m thick Vibratome sections were prepared. Sections were first incubated in 50% ethanol (in PBS) for 30 minutes, followed by 15 minutes in 3% H₂O₂ (in PBS). Following a PBS rinse the sections were incubated in 10% Normal Donkey Serum (NDS) in TNB (NEN Cyanine-3 TSA System, NEL) for 10 minutes. Sections were rinsed in PBS and incubated overnight in primary antibody (chicken α - β -galactosidase, 1:500; rabbit α -S100B 1:2000] in TNB with 3% NDS overnight at 4°C. Following a wash in TNT solution (NEN Cyanine-3 TSA System, NEL; 5' x3) the section were incubated with AMCA-conjugated donkey anti-chicken (1:200) and FITC-conjugated donkey anti-rabbit (1:200) in TNB with 3% NDS for 2 hours at room temperature. Sections were then rinsed in TNT (5' x3) and PBS (2' x2) and incubated in M.O.M. blocking reagent for 1 hour at room temperature. Sections were rinsed in PBS (2' x2) and then preincubated in M.O.M. diluent (5') followed by mouse anti-NeuN (1:100) in M.O.M. diluent for 30 minutes. Following a PBS rinse (2' x2) NeuN staining was visualized by incubating with M.O.M. anti-mouse biotin-conjugated reagent (1:250 in M.O.M. diluent) for 10 minutes, then AlexaFluor555 Streptavidin (1:50) in PBS for 10 minutes. For the double immunofluorescence in figures 1I to 1K 50 μ m Vibratome sections were incubated in 50% ethanol (in PBS) for 30 minutes, followed by 10 minutes in 3% H₂O₂ (in PBS). Following a PBS rinse the sections were incubated in 10% Normal Goat Serum (NGS) in TNB for 30 minutes. Sections were rinsed in PBS and incubated overnight in rabbit α -GAD67 (1:1500) in TNB with 3% NGS overnight at 4°C. Following a wash in TNT solution (5' x3) the section were incubated with biotinylated goat anti-rabbit (1:200 in TNB with 3% NGS) for 2 hours at room temperature. Following a TNT rinse (5' x3) sections were placed in ABC solution for 30 minutes and then visualized with Cyanine-3 Tyramide (1:50) for 5 minutes. Sections were rinsed in TNT (5' x3) then incubated in 3% NGS in TNB for 10 minutes. β -galactosidase-IR was visualized by incubating the sections in rabbit anti- β -galactosidase (1:2000 in TNB/3% NGS) at 4°C overnight. Following a TNT rinse (5' x3) staining

was visualized with AlexaFlour488 conjugated goat anti-rabbit (1:200 in TNB/3% NGS) at room temperature for 2 hours. The β -gal/BrdU double immunostaining was also conducted on 50 μ m free floating sections prepared from 4% PFA perfused mice. 24 hours prior to perfusion the animals received a series of intraperitoneal injection of BrdU (1 injection/day for 12 days; 10mg/ml in 0.9%NaCl/0.007N NaOH at 50 μ g/g of body weight). Following anti- β -gal staining as described above, sections were incubated in 0.6% H₂O₂ in TBS for 30 minutes, followed by 2N HCl at 37 °C for 30 minutes. Sections were placed in 0.1M Boric Acid (pH 8.5) for 10 minutes and then rinsed in TBS (5' x2). Following blocking in M.O.M. blocking reagent for 30 minutes sections were placed in mouse anti-BrdU (Roche, 1:400 in M.O.M. diluent) overnight at 4°C. The next day sections were rinsed in TBS (2' x2) and placed in biotin-conjugated anti-mouse M.O.M. reagent for 30 minutes and the signal was amplified with the ABC system and visualized with AlexaFlour488 streptavidin.

For the anti-NR1 staining in Fig. 2 brains were removed following perfusion and embedded in paraffin. Coronal sections (8 μ m thick) were prepared. The slides were first dewaxed and rehydrated (Xylene for 5' x2; 100% ethanol for 5' x2; 95% ethanol for 3'; 70% ethanol for 3', 50% ethanol for 3'; running tap water for 5'). Following 2' incubation in PBS, the sections were pretreated with 3% H₂O₂ in PBS for 15' and then again rinsed in PBS (5'x2). Next the slides were warmed to 37°C and submerged in 0.2N HCl containing 1mg/ml Pepsin at 37°C for 10'. Slides were rinsed in PBS (5'x3) then submerged in 10% NDS in TNB for 30'. Following a rinse in TNT buffer (5'x3) the section were incubated in anti-NR1 (1:100 in TNB/3% NDS) overnight at room temperature in a humidified chamber. The next day sections were rinsed in TNT (5' x3) and incubated with biotin-conjugated donkey anti-rabbit (1:200 in TNB/3% NDS) for 2 hours at room temperature. Signal was first amplified by incubating in ABC solution for 30 minutes and then visualized by incubating in AlexaFlour488 tyramide (1:100) for 7 to 10 minutes. Images were collected with a SPOT camera and epiflourescent illumination. β -gal/BrdU double staining image was collected with a confocal laser scanning microscope.

In situ Hybridization

In situ hybridization was carried out as described in Nakazawa et al. (4). In brief, brains were removed and frozen fresh in OCT solution. 10 µm parasagittal sections were prepared in a cryostat and mounted onto pre-coated glass slides. Sections were post fixed with 4% paraformaldehyde in PBS for 15 min, and treated with 10 µg/ml proteinase K at 37°C for 30 min followed by 0.2 M HCl for 10 min. After rinsing, sections were further incubated in 0.25% acetic anhydride and 0.1 M triethanolamine for 10 min to avoid non-specific binding of the probe. Following dehydration with ethanol, hybridization was performed at 55°C for 18 hours in a hybridization buffer containing 50% formamide. For detection of the mouse NR1 mRNAs, a complementary RNA (cRNA) probe, derived from the AvrII-SphI 0.4-kb antisense DNA fragment of rat NR1 cDNA containing from exon 13 to exon 16 (5), was labeled with [33P]UTP (5x10⁵ cpm), and added to the hybridization buffer. The brain sections were serially washed at 55°C with a set of SSC buffers of decreasing strength, the final strength being 0.2x and then treated with RNase A (12.5 µg/ml) at 37°C for 30 min. The sections were exposed to hyper-beta max for 2 days and were dipped in nuclear emulsion followed by exposure to X-ray film for 3-4 weeks. Images were collected with a SPOT camera attached to a microscope.

Timms Staining

Mice were first transcardially perfused with buffered Na₂S solution (11.9g NaH₂PO₄•H₂O; 3.7g Na₂S•9H₂O; 1L ddH₂O) for 10 minutes, followed by 4% PFA in 0.1M PB (pH 7.5) for 10 minutes, then the brains were removed and post-fixed in 4% PFA overnight. 50 µm thick sections were cut on a Vibratome, collected in PB and mounted on gelatin coated slides. Developer solutions (Solution A: 144mL ddH₂O, 72g Gum Arabic; Solution B: 6.99g Citric Acid monohydrate, 7.05g Sodium Citrate•2H₂O, add ddH₂O to 30mL; Solution C: 2.55g Hydroquinone, ddH₂O to 45mL; Solution D: 0.3375g AgNO₃, ddH₂O to 45mL) were prepared. Developer solutions are mixed in the dark room and following a brief rinse in ddH₂O slides are placed in the

developing solution for 60 minutes. Following developing slides are rinsed in ddH₂O and cleared with ethanol/xylene treatment.

In vivo Synaptic Plasticity

In vivo LTP experiments were performed in urethane-anesthetised male DG-NR1 KO mice and *f*NR1 littermate controls (age 20-24 weeks) using 'LTP' software with the experimenter blind to the genotype of the animals (6). Stimulation of the perforant path (concentric bipolar electrode, 100 μ s pulses) evoked field potentials in the hilus of the ipsilateral DG. Initial field EPSP slope and population spike amplitude were used to quantify pp-DG synaptic efficacy and granule cell responses respectively. Input-output relationships (10-500 μ A) and paired-pulse facilitation (inter-stimulus intervals of 10-1000ms) were tested prior to LTP induction by 6 series of 6 trains of 6 pulses at 400Hz (100ms between trains, 20s between series). LTP was expressed relative to 20 pre-tetanus control responses (1 per 30s at a stimulation intensity just above threshold for evoking a population spike). In a separate set of experiments, stimulating and recording electrodes were placed in CA3 and stratum radiatum of contralateral CA1 respectively. Following a control period of test responses (at a stimulation intensity that evoked a 50% maximal field EPSP slope), LTP of Schaffer collateral-pyramidal cell synapses was induced using 3 trains of 50 pulses at 100Hz (30s between trains).

One-trial contextual fear conditioning and generalization

These experiments were conducted at MIT's Picower Institute for Learning and Memory. The mice were housed in plastic homecages with laboratory bedding (2-4 mice/cage) and had *ad libitum* access to food and water with a 12:12 hour light/dark cycle. Shocking and testing were conducted in dedicated behavioral training rooms located in the animal facility during the light cycle. All experiments were conducted and analyzed by scientists blind to the genotypes of the

animals. 12 male mice of each genotype (DG-NR1 KO and ν NR1 littermate controls) between 16 and 24 weeks of age were transported from the behavioral colony to a holding room adjacent to the behavioral suite containing the fear conditioning chambers where they sat undisturbed for thirty minutes prior to the experiment. On Day 1 mice were brought into a room lit with overhead fluorescent lighting and containing four conditioning chambers. The chambers had plexiglass fronts and backs and aluminum side walls, and measured 30 x 25 x 21 cm. The chamber floors consisted of 36, 3.2 mm diameter stainless steel rods spaced 7.9mm apart connected via a cable harness to a shock generator. The chambers were cleaned between mice with 70% ethanol and a solution of 1% acetic acid was placed beneath the chambers during the experiment to provide an olfactory cue. All experiments were conducted using FreezeFrame software. Once placed in the chamber the mice were allowed to freely explore for 3 minutes, then received a single, unsignaled 0.75mA footshock (2 sec in duration). Following the shock the mice remained in the chamber for one minute. At the conclusion of the session they were returned to their home cages and transported back to the holding room. On Day 2 the mice were returned to an adjacent conditioning room lit with dim red light and placed into chambers measuring 30 x 25 x 21 cm with a plexiglass front and back and aluminum side walls. However, these chambers contained a white, curved plastic roof and a smooth, white plastic floor. Extensive pilot testing had demonstrated that the replacement of a metal grid with the plastic floor prevented the generalization of the freezing response following single shock conditioning (T. McHugh, unpublished). In addition, the odor in the pan beneath the chamber was switched to 0.25% Benzaldehyde (in 100% EtOH) to further alter the context. Freezing in this chamber was assessed for 5 minutes. On day 3 the mice were returned to the original conditioning chambers (identical to Day 1) for a five minute test. During all sessions the animal's activity in the chamber was recorded using FreezeFrame software. Freezing behavior was assessed from the video image of the mouse using FreezeView software, with a minimum bout time of 2 seconds. Freezing values were then averaged over mice of a particular genotype for each session.

Contextual Fear Discrimination Task

Twenty-two male mice between 16 and 24 weeks of age (11 DG-NR1 KO and 11 *f*NR1 littermate controls) were used in this experiment conducted in the UCLA Department of Psychology. All experiments were conducted and analyzed by scientists blind to the genotypes of the animals. The mice were allowed several weeks to acclimate following shipment from MIT to UCLA. The mice were housed in plastic tubs with laboratory bedding (4 mice/tub), had *ad libitum* access to food and water, and lived on a 12:12 hour light/dark cycle. All procedures occurred during the light cycle.

In this experiment there were two important procedural differences from the one-trial fear task. First, as detailed below, the mice received three days of conditioning in Context A before the discrimination phase of the task began, allowing for greater generalization in both genotypes of mice. Second, in this task both chambers had identical grid floors, which pilot studies in the Fanselow laboratory had shown to be important for the generalization of the fear memory. Mice were trained to discriminate between two contexts through repeated experience in each. Context A consisted of four identical conditioning chambers (28 X 21X 21 cm). The side walls of each chamber were made of aluminum while the front door, back wall, and ceiling were made of clear Plexiglas. The floor of each chamber consisted of 33 stainless steel rods, separated by 6 mm, which were wired to a shock generator and scrambler. A stainless steel pan coated with benzaldehyde in 100% alcohol (0.25% concentration) was placed under the grid floor in each box to provide a distinct odor. Each chamber was cleaned thoroughly with an odorless 5% sodium hydroxide solution before the animals were placed in the chambers. A fan located inside the room provided background noise at 65 dB. The overhead fluorescent room lights remained on. Context B consisted of four chambers in which the white Plexiglas side walls sloped inward at a 60° angle from the floor (28 X 21 X 21 cm). As in context A, the floor of each chamber consisted of 33 stainless steel rods, separated by 6 mm, which were wired to a shock generator and scrambler. This context was cleaned and scented with a 1% acetic acid solution. A white noise

generator provided the 65 dB background noise. The room was lit with a 30-W red overhead light and a 30-W red light located in the corner of the room opposite the chambers. Animals were tail marked approximately every seven days beginning one day prior to conditioning to allow for within-tub identification. Each day, the animals were transported in their home tubs to a room adjacent to the experimental room. They were left undisturbed for at least 20 min. On days 1-3 the mice were carried to the A-context conditioning room in their home tub and placed into the conditioning chambers. After 192sec, they received a single footshock (2 sec; 0.65mA) and were removed from the chambers 1min following footshock termination. Across the subsequent two consecutive days (days 4 and 5), mice were placed into the A-context and B-context conditioning chambers in separate tests (counterbalanced order). Each test consisted of an 8min exposure to the chamber without the delivery of footshock. On days 6 through 17 (which began the day after the second test above), mice were exposed to both A-context and B-context conditioning chambers daily. The order of exposure on each day followed a BAABABBABAAB design such that on days 7, 8, 10, 13, 15 and 16 all animals were exposed to Chamber A first and Chamber B second. For the remaining days, the order was reversed. Across the entire discrimination phase, all animals received a single footshock during each Chamber A exposure and never received footshock during Chamber B exposures. The dependent measure employed was freezing behavior, defined as behavioral immobility except for movement necessary for respiration (7). An observer, blind to the genotypes of the mice, scored each mouse as either freezing or not freezing every 8 sec for the duration of each 8 min context test that occurred following the first 3 days of acquisition. On each subsequent discrimination day (days 6 to 17) each animal was scored every 8 sec for the first 192 sec in each context on each day. These scores were then converted into a percentage of observations spent freezing. Discrimination ratios were calculated for discrimination phase using these freezing percentage scores according to the following formula: Chamber A/(Chamber A + Chamber B).

In vivo Recording

Male mice (DG-NR1 KO and *f*NR1 littermate controls, 16-24 weeks of age) were implanted with a microdrive array consisting of six independently adjustable tetrodes (for CA1 recordings: stereotaxic coordinates from bregma: 1.6 mm lateral; 1.8 mm posterior; for CA1/CA3 recordings: 1.6mm lateral; 1.4 mm posterior) as previously described (8). All experiments were conducted and analyzed by scientists blind to the genotypes of the animals. On the day prior to the start of the experiment the animals were allowed to forage for small chocolate pellets randomly scattered in a novel white, circular, low walled open field arena (48 cm in diameter) placed in the center of a table in a curtained section of a quiet recording room. Diffuse room lighting was provided by low intensity spotlights focused onto four salient visual cues located on each of the walls of the recording chamber. On the next day we began the experiment. The pattern separation recording sessions consisted of two "RUN" epochs (10 min each) bracketed by 20 minute "SLEEP" sessions in which the animal rested quietly in a small high-walled box outside of the behavioral environment. The first recording session, "RUN 1", was conducted in the same white, circular, low walled open field arena, again placed in the center of a table in the recording room. Prior to the second recording session, "RUN 2", we exchanged the white circular arena for a black, square, low walled open field (43 cm x 43 cm). During RUN2 the mouse was placed in the black square and again allowed to randomly forage for chocolate reward for 10 minutes. As animals explored the open field arenas extracellular action potentials were recorded while the animal's position was tracked using a pair of infrared diodes placed 3 cm above the animals head. Subsets of the mice were returned to the recording room the following day and the experiment was repeated in an identical manner. At the conclusion of the experiment mice were given a lethal dose of anesthetic and a small electrical current (50 μ A) was run down each tetrode for 8 seconds to create a small lesion at the tip of the probe. Animals were then transcardially perfused with 4% paraformaldehyde (PFA) in 0.1 M sodium phosphate buffer (PB) and brains were removed. We prepared and mounted 50 μ m Vibratome which were counterstained with Nuclear Fast Red.

Recording position of each tetrode was verified by examining the location of the lesions under standard light microscopy.

Following data acquisition, action potentials were assigned to individual cells based on a spike's relative amplitudes across the four recording wires of a tetrode (Fig. S3) (8). Additionally, cells were only included in the rate remapping analysis if the following conditions were met: 1) a relatively broad waveforms ($> 350 \mu\text{s}$) 2) a peak firing rate greater than 5 Hz, and 3) a Complex Spike Index (a measure of bursting- see below) of greater than 5%. Additionally, for the units to be included in the rate remapping analysis the following conditions must be met: 1) the waveform profiles of isolated cells had to remain stable across the 20 minute delay between recording sessions and 2) cells had to have an average firing rate of at least 0.2 Hz in one of the contexts. To characterize the consequences of the loss of NRs in the GCs on the activity of the CA1 and CA3 pyramidal cells we measured several properties including: 1) the Complex Spike Index (CSI)- defined as the percentage of spikes with first lag interspike intervals between 2 & 15 ms and whose second spike is smaller in amplitude than the first, 2) average and peak firing rates, 3) spike width (peak to trough) and 4) place field size, expressed as the percent of sampled pixels in which the mean firing rate of the cell exceeded 0.5 Hz. To assess the similarity of the ensemble activity during RUN1 and RUN2 of the pattern separation recording sessions for each pyramidal cell meeting our minimum criteria we calculated, on a cell by cell basis, two measures of rate remapping: 1) the Rate Difference ($((\text{high rate}-\text{low rate})/(\text{high rate}+\text{low rate}))$) and 2) the Rate Overlap ($(\text{high rate}/\text{low rate})$) (9-11). Rate Differences for each hippocampal region and recording day were then averaged over mice of a particular genotype. These values were compared to estimated Rate Difference values expected from independent firing rates in each region. To generate these we used a bootstrap method, substituting RUN2 values of each unit with values randomly drawn from the actual rates recorded in the corresponding region and genotype during RUN1 or RUN2 and calculating the Rate Difference. This procedure was repeated 10000 times to generate an average and standard deviation value for each region. We then calculated a Z-score

for the actual Rate Difference observed in each region and genotype. To calculate the changes in place field positions in the two contexts, we divided the arenas into pixels of approximately 4cm by 4cm and for each pixel calculated an average firing rate for each 10 minute RUN session. We then aligned the centers of the two boxes and calculated the distance between peak firing rate pixels in RUN1 and RUN2. Distances were then averaged across region and genotype.

2. Supporting Text

Time line of the loss of NR1 RNA in the DG.

In situ hybridization was performed on DG-NR1 KO and *f*NR1 littermates at a series of ages (1.5 weeks, 4 weeks, 12 weeks, 16 weeks, and 24 weeks) to determine the kinetics of the NR1 mRNA loss in the DG of the mutant mice (Fig. S1). At postnatal 1.5 weeks the level of NR1 mRNA in the DG of the mutant mice is indistinguishable from the littermate controls. At postnatal 4 weeks the NR1 mRNA is detected abundantly in the DG GCs in the mutant mice, although a slight reduction can be observed. NR1 RNA is nearly absent by 16 weeks of age in the DG GC layers. The low levels of NR1 mRNA signals observed in the space between the blades of the DG in the 16 week and 24 week mutants are presumably due to the lack of NR1 knockout in the inhibitory neurons (see Fig. 1I to 1K). This pattern of NR1 mRNA level remained until at least 24 weeks of age.

Open field activity.

To assure the mutant mice did not possess any change in baseline exploratory behavior the mice were tested for motor behaviors with the use of an automated Digiscan apparatus (Accuscan Instruments, Columbus, OH) in which activity is measured by IR beam interruption. Horizontal activity, measured as the total distance traveled by each mouse, was recorded in 1-min intervals over a 10-min period in 18 male mice of each genotype (DG-NR1 KO and *f*NR1 littermate controls, aged 16-24 weeks) in a novel chamber. Data collected was averaged across the 1-minute

interval by genotype. All experiments were conducted and analyzed by scientists blind to the genotypes of the animals. As seen in Fig. S2A we observed no difference in activity between the control and mutant mice (2-way ANOVA, Genotype x Minute, $F(1,9) = 1.084$, $p = 0.37$; Genotype, $F(1,9) = 0.04$, $p = 0.84$; Minute, $F(1,9) = 8.9$, $p < 0.0001$).

Body weight and feeding behavior.

To assess the possible consequences of an undetectable decrease of NR function in the arcuate nucleus we monitored the body weight and response to starvation, phenotypes known to be sensitive to arcuate function, in control and mutant mice (12, 13). A 15-week longitudinal study of 14 male DG-NR1 KO mice and 14 male *f*NR1 littermate controls was conducted beginning at postnatal week 10. All experiments were conducted and analyzed by scientists blind to the genotypes of the animals. We observed no differences in the body weight across this time period (Fig. S2A). In a second group of male mice ($n=8$ DG-NR1 KO, $n=8$ *f*NR1 littermate controls) we measured the free feeding body weight at 26 weeks of age and again found no difference (Fig. S2B). These mice were then subjected to a 24 hour starvation and body weight was assessed the next day. Both genotypes were found to have lost similar amounts of weight (Fig. S2C). Following this starvation period we allowed the mice free access to standard mouse chow and measured the amount consumed in a 2 hour period. There was no significant effect of genotype on the food consumed during this recovery period (Fig. S2D).

Morris water maze.

To assess the spatial learning ability of the DG-NR1 KO mice we subject them to a reference memory version of the Morris water maze (14). 6 male DG-NR1 KO mice (16-20 weeks of age) and 6 male *f*NR1 littermate controls were given four training trials (60 seconds maximum; 1 hour ITI) daily to locate a small (12 cm) platform hidden 2-cm below the surface of a milky-white pool of water (1.6m in diameter; Data collected with HVS Image Water 2020 software) using only

distal cues in the surrounding room. Both genotypes demonstrated similar acquisition of the task over fifteen days (Genotype x Day $F(1,14)=0.73$, $p=0.74$; Day $F(1,14)=18.33$, $p<0.0001$; Genotype $F(1,14)=0.08$, $p=0.78$). One hour following the final training trial on Day 15 the platform was removed from the pool and the mice were allowed to swim for 60 seconds in a probe trial. This probe trial detected no difference in target quadrant search preference between the genotypes (fNR1 Target x Opposite $p<0.001$; DG-NR1 KO Target x Opposite $p<0.001$).

Intra-run changes in rate difference and shift of peak firing location in CA3.

To assess the stability of the CA3 place cells we have compared the average firing rates of individual CA3 cells during the first half of RUN1 (RUN1a) in the circular arena and the second half of RUN1 (RUN1b), as well as those during the first and second halves of RUN2 (RUN2a and RUN2b, respectively). Analyses of these intra-run rate differences indicated similar values in both genotypes and in both RUN1 and RUN2. Furthermore, a repeated measure 2-way ANOVA of all the Rate Difference data (RUN1a:RUN1b, RUN1:RUN2, RUN2a:RUN2b) data revealed a significant interaction of genotype and session ($F(1,2) = 0.12$, $p=0.0006$; Fig. S5A) and Bonferroni post-tests reveal that only in the control mice is there a significant increase in rate difference in the RUN1:RUN2 condition when compared to the intra-run data (fNR1 CA3: RUN1a:RUN1b x RUN1:RUN2 $p<0.001$, RUN2a:RUN2b x RUN1:RUN2 $p<0.001$; DG-NR1 KO RUN1a:RUN1b x RUN1:RUN2 $p>0.05$, RUN2a:RUN2b x RUN1:RUN2 $p>0.05$). Thus, the place fields in control mice during both RUN1 and RUN2 were stable enough to reveal the significant effect of the context shift on the firing rates. Furthermore, there was no significant effect of the mutation on the intra-run rate differences between RUN1a and RUN1b or between RUN2a and RUN2b (Bonferroni post-test RUN1a:RUN1b Control x Mutant $p>0.05$; RUN2a:RUN2b Control x Mutant $p>0.05$), indicating the mutants' place fields are no more unstable than the controls' place fields. Similarly, the shift in the peak firing location was

equivalent in the controls and mutants across a single run session (RUN1a and RUN1b or RUN2a and RUN2b; Fig. S5B), and while there was an effect of session, a 2-way ANOVA and post-test found no genotype differences (Genotype x Session $F(1,2)=0.19$, $p=0.83$, Genotype(1,2)=0.04, $p=0.84$, Session $F(1,2)=3.9$, $p < 0.03$). Since individual cells do show significantly lower rate changes (at least in the control mice) and lower peak firing location shifts across individual run sessions, as compared to between them, the alterations we see between RUN1 and RUN2 reflect specific context-dependent changes in ensemble activity, not slow refinement of noisy spatial coding.

Measurement of cluster quality.

To ensure there were no systematic difference in the quality of isolation of the clusters between the two genotypes of mice we conducted cluster quality measurements using the Mahalanobis distance measure in full 12-dimensional space (15). As seen in Table S2 we found no significant differences between the genotypes in either CA1 ($p = 0.28$) or CA3 ($p = 0.15$). Example of typical unit isolations can be seen in Fig. S3.

3. Supporting Figures

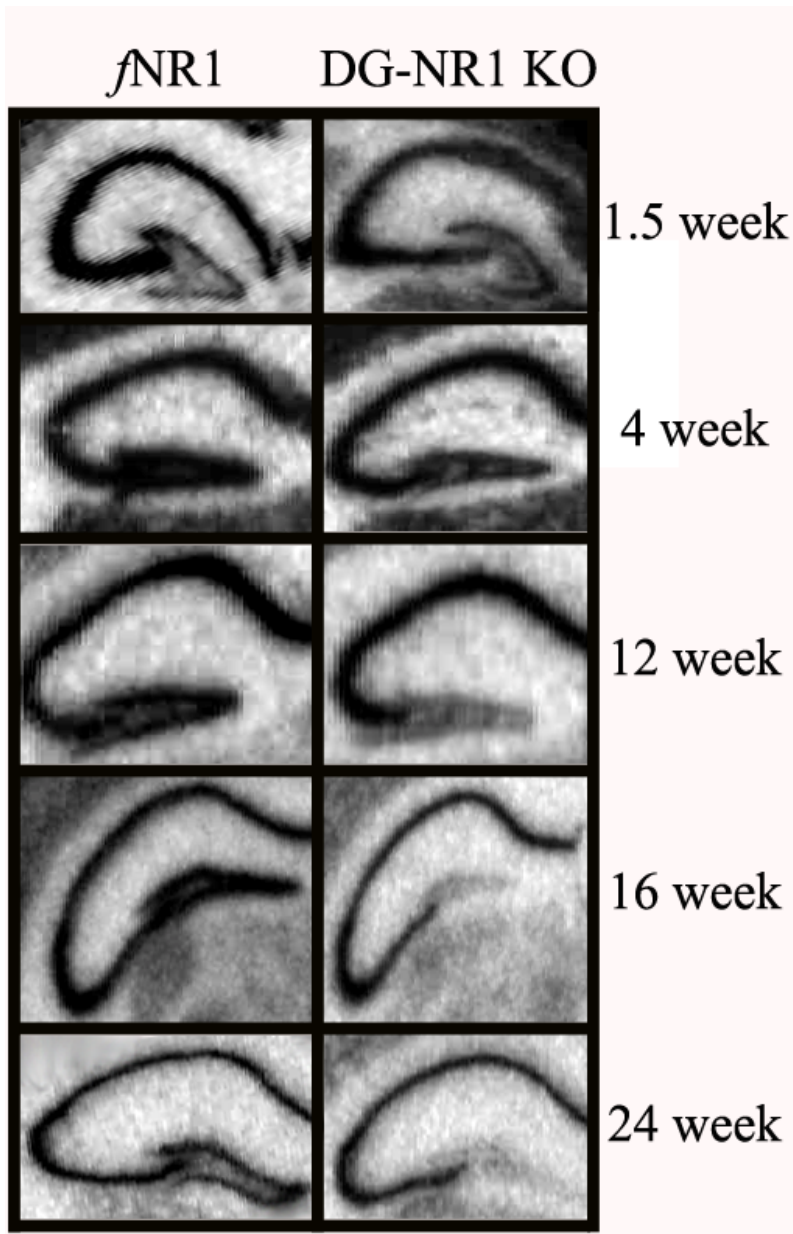


Fig. S1: Developmental kinetics of the loss of the NR1 mRNA in the DG-NR1 KO mice. *In situ* hybridization with a ^{33}P -labeled NR1 cDNA probe on f NR1 control mice (left column) and DG-NR1 KO littermates (right column) at four developmental time-points. At postnatal 1.5 weeks the level of NR1 mRNA is normal in the DG of the mutant mice. But, at postnatal 4 weeks a decrease can be detected, at 12 weeks NR1 mRNA is noticeably reduced and at 16 weeks is nearly absent. This pattern remains stable until at least postnatal 24 weeks. The low levels of hybridization signals observed between the blades of the DG are presumably due to NR1 gene expression in inhibitory neurons.

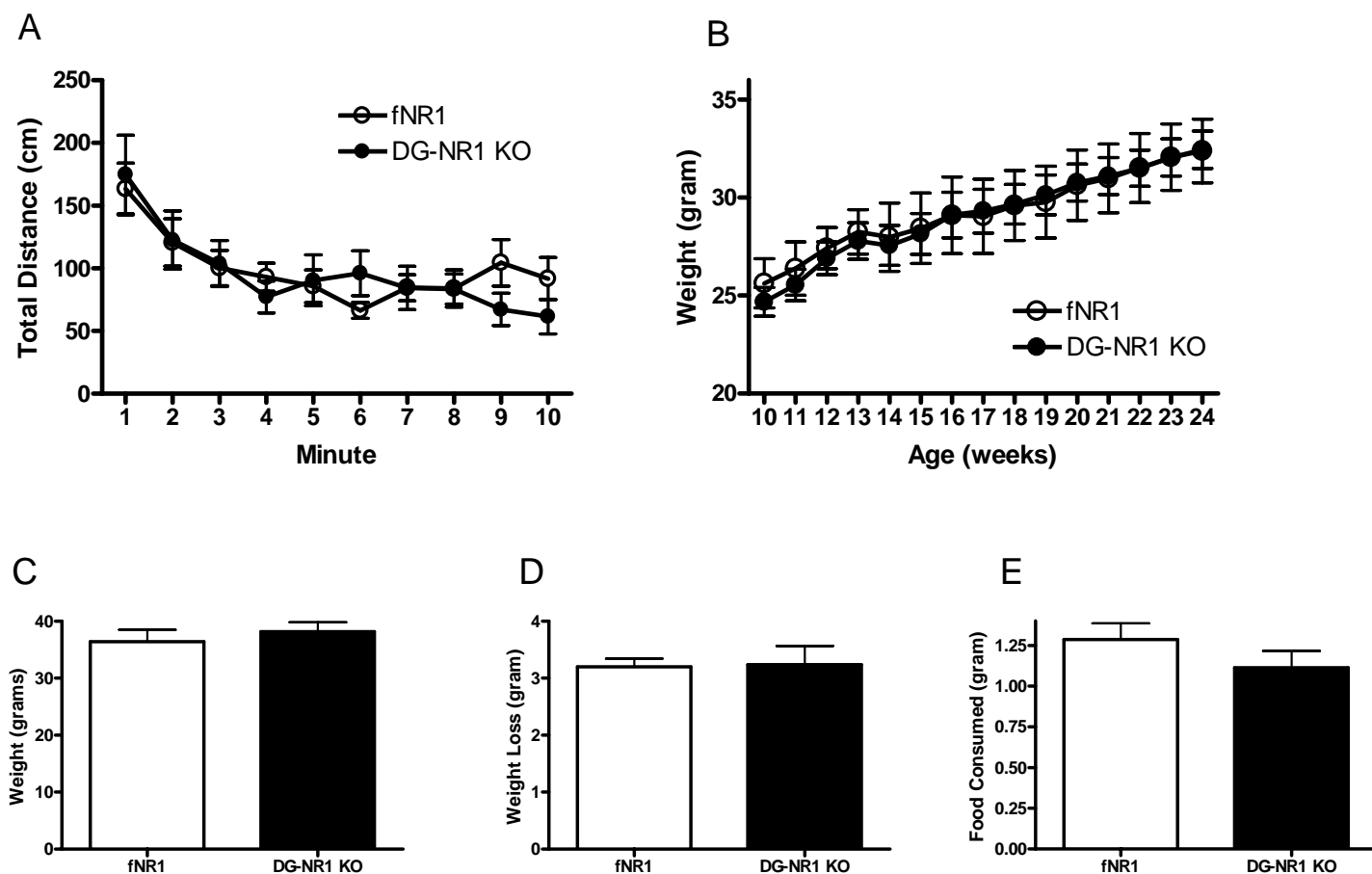


Fig. S2: DG-NR1 KO mice exhibit no changes in activity, body weight, or feeding behavior. (A) Total distance traveled in a novel open field chamber across a 10 minute session is similar in fNR1 and DG-NR1 KO mice (2-way ANOVA, Genotype x Minute, $F(1,9) = 1.084$, $p = 0.37$; Genotype, $F(1,9) = 0.04$, $p = 0.84$; Minute, $F(1,9) = 8.9$, $p < 0.0001$). (B) A longitudinal study of body weight in male fNR1 and DG-NR1 KO mice reveals no significant differences (2-way ANOVA, Genotype x Week, $F(1,14) = 0.05$, $p = 1.0$; Genotype, $F(1,9) = 0.11$, $p = 0.73$; Week, $F(1,9) = 5.5$, $p < 0.0001$). (C) The free feeding body weight of male mice at 26 weeks of age was similar in the genotypes (fNR1 = 36.4g, DG-NR1 KO = 38.2g; $p = 0.51$) (D) Following 24 hr starvation the genotypes demonstrated equivalent weight loss (fNR1 = 3.2g, DG-NR1 KO = 3.2g; $p = 0.92$) and (E) showed similar food consumption (fNR1 = 1.3g, DG-NR1 KO = 1.1g; $p = 0.26$) during a 2 hr recovery period.

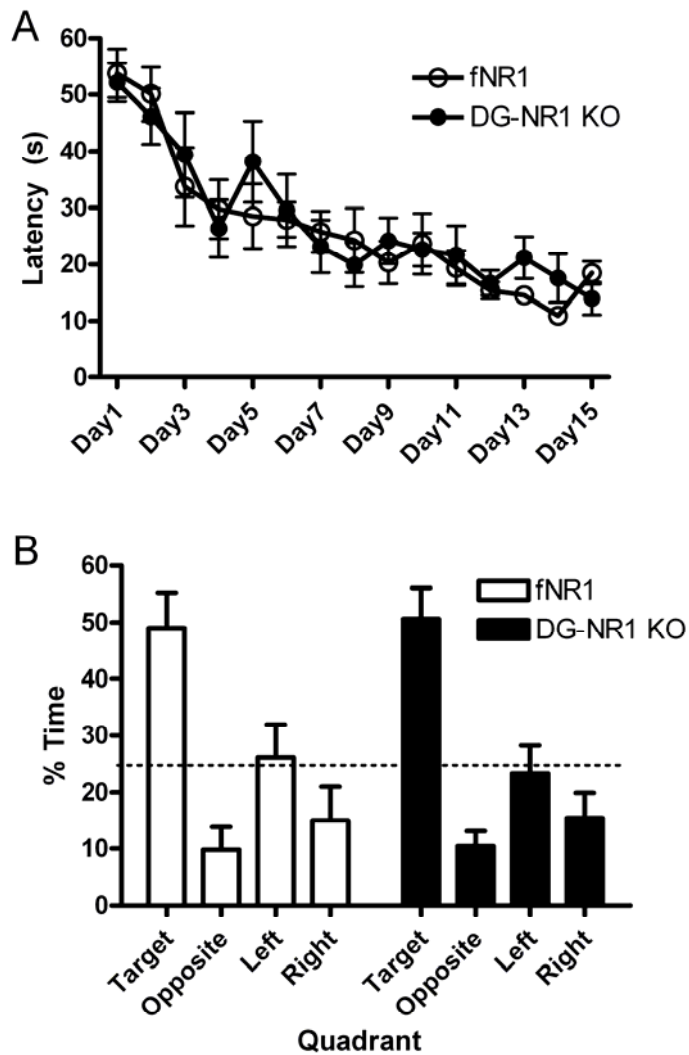


Fig. S3: DG-NR1 KO mice exhibit no deficit in the reference memory version of the Morris water maze. (A) There was no significant difference between the genotypes in the average latency to locate the hidden platform across fifteen days of training (Genotype x Day $F(1,14)=0.73$, $p=0.74$; Day $F(1,14)=18.33$, $p<0.0001$; Genotype $F(1,14)=0.08$, $p=0.78$) (B) A probe trial on Day 15 detected no difference in target quadrant search preference between the genotypes (fNR1 Target x Opposite $p<0.001$; DG-NR1 KO Target x Opposite $p<0.001$).

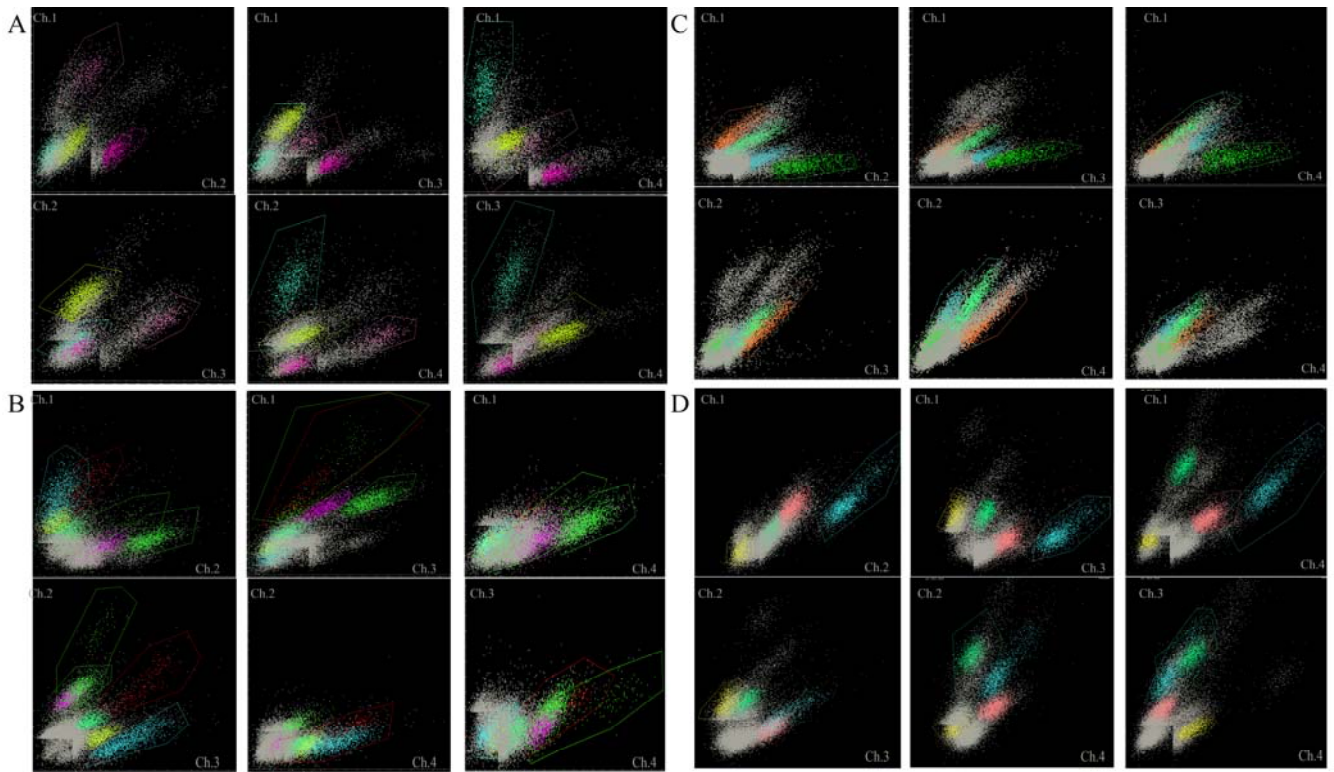


Fig. S4: Representative recording of ensemble activity in the CA1 and CA3 regions of fNR1 and DG-NR1 KO mice. Multidimensional cluster diagrams illustrating spike isolation of units recorded in the CA1 and CA3 regions of both fNR1 and DG-NR1 KO mice. The scatter plots show the relationship of amplitudes of spikes recorded from the 4 channels of each tetraode. Color-coded clusters are likely to include spikes from the same pyramidal unit. (A) Four simultaneously recorded units in the CA1 region of a fNR1 mouse, (B) four simultaneously recorded units in the CA1 region of a DG-NR1 KO mouse, (C) four simultaneously recorded units in the CA3 region of a fNR1 mouse, and (D) four simultaneously recorded units in the CA3 region of a DG-NR1 KO mouse.

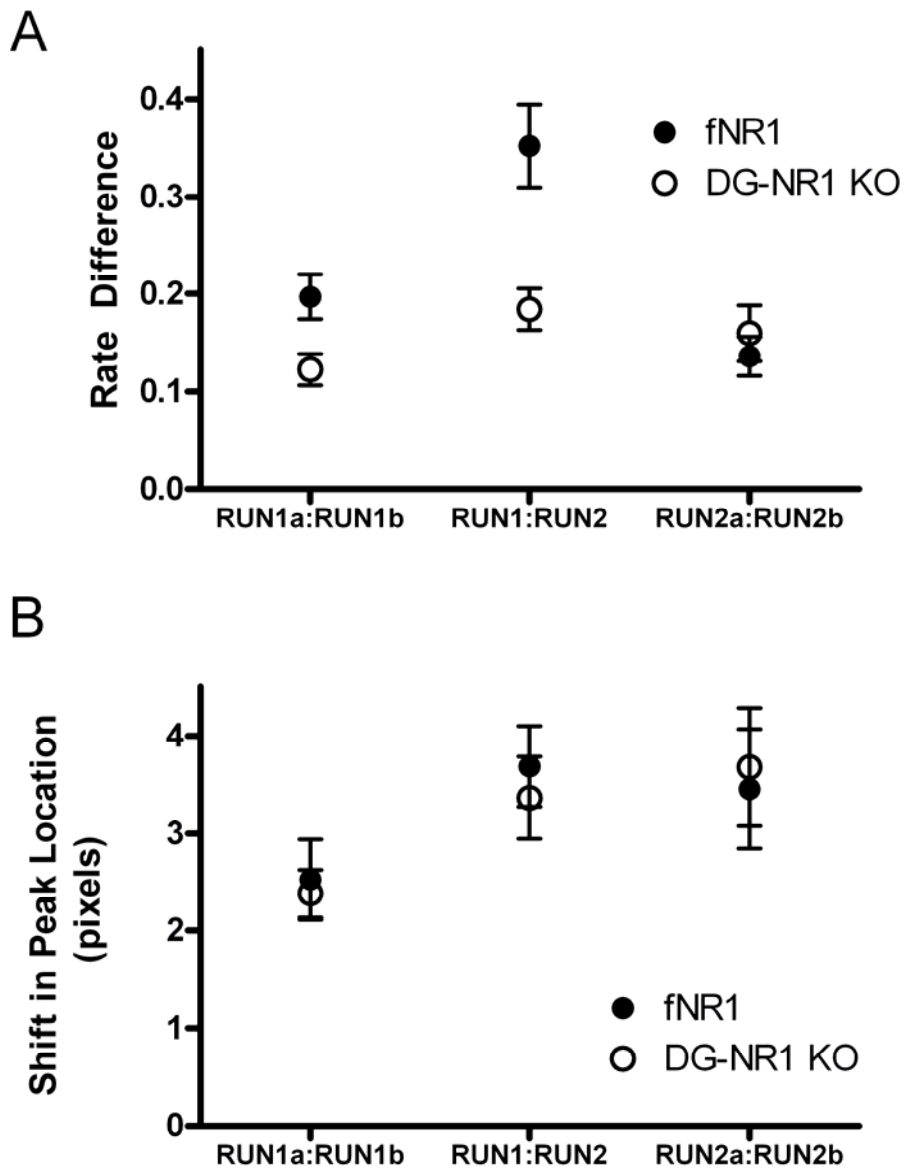


Fig. S5: Intra-run vs inter-run rate difference and shift in peak locations in CA3. (A) Intra-run rate difference was calculated for both RUN1 (RUN1a:RUN1b) and RUN2 (RUN2a:RUN2b) and found to be similar in both genotypes. Compared to the inter-run rate change (RUN1:RUN2) we found a significant interaction of genotype and session (Genotype x Session $F(1,2) = 0.12, p = 0.0006$). (B) Similar analysis of the shift in the location of the peak firing rate of each cell found no effect of genotype.

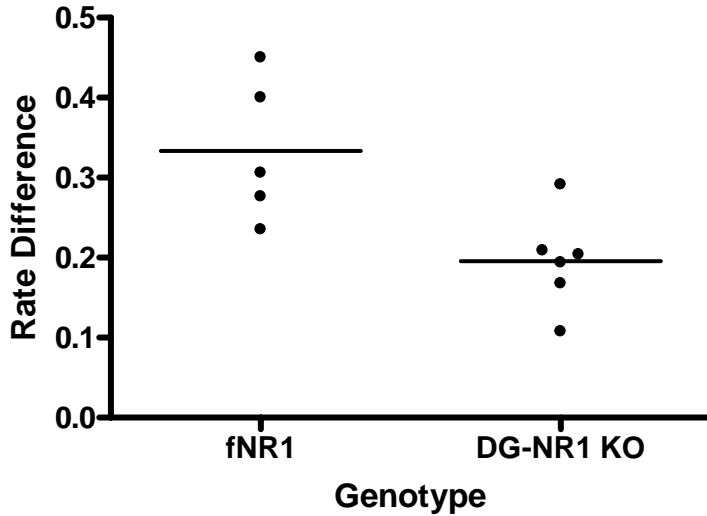


Fig. S6: Reduced rate difference in the CA3 region of the DG-NR1 KO mice. Each point represents the average rate difference of a single animal of the indicated genotype, the line indicates the group mean. Averages and number of cells contributed by each mouse is listed in Table S1 (t-test, $p < 0.02$).

4. Supporting Tables

f/NR1

Mouse	# of CA3 Cells	RATE DIFFERENCE
K4601	1	0.276520717
K4423	9	0.450330521
K4595	5	0.235178547
K4616	3	0.400134266
K4638	8	0.306013007

DG-NR1 KO

Mouse	# of CA3 Cells	RATE DIFFERENCE
K4617	2	0.209042749
K4545	4	0.291331248
K4607	2	0.203877619
K4596	6	0.10779871
K4647	7	0.167553962
K4634	5	0.193758278

Table S1. Table indicates the contribution of the individual animals to the rate differences calculated for each genotype.

*f*NR1

		Average Rate (Hz)	Peak Rate (Hz)
Cell 1	Circle	0.27	13.00
	Square	0.34	24.00
Cell 2	Circle	0.28	16.20
	Square	0.08	3.50
Cell 3	Circle	0.23	22.50
	Square	0.12	24.20
Cell 4	Circle	0.32	8.30
	Square	1.00	22.00
Cell 5	Circle	0.93	9.40
	Square	0.36	10.90
Cell 6	Circle	0.55	9.80
	Square	0.19	6.70
Cell 7	Circle	1.10	33.80
	Square	1.40	14.60
Cell 8	Circle	1.20	11.30
	Square	0.21	6.40
Cell 9	Circle	0.06	5.80
	Square	0.32	15.50
Cell 10	Circle	0.14	9.00
	Square	0.31	25.40

DG-NR1 KO

		Average Rate (Hz)	Peak Rate (Hz)
Cell 1	Circle	1.00	30.00
	Square	0.91	21.90
Cell 2	Circle	1.00	19.20
	Square	0.78	30.00
Cell 3	Circle	0.32	8.30
	Square	0.43	11.30
Cell 4	Circle	0.71	19.20
	Square	0.62	19.30
Cell 5	Circle	0.23	11.30
	Square	0.24	17.20
Cell 6	Circle	0.20	10.30
	Square	0.10	10.90
Cell 7	Circle	0.24	12.40
	Square	0.14	12.60
Cell 8	Circle	0.23	10.60
	Square	0.17	13.70
Cell 9	Circle	0.26	12.60
	Square	0.16	6.50
Cell 10	Circle	0.31	12.90
	Square	0.41	20.90

Table S2. Firing rate information for example fields in figure 5A. For each cell the average and peak firing rate for each environment is listed to the right.

	CA1	CA3
DG-NR1 KO	19.78 ± 0.95	20.92 ± 1.90
fNR1	22.72 ± 2.12	34.30 ± 8.50

Table S3. Cluster quality measurements using the 12-d Mahalanobis distance measure. We found no significant differences in the average cluster quality between the cells recorded in CA1 or CA3 of the fNR1 and DG-NR1 KO mice.

5. Supporting References

1. N. Balthasar *et al.*, *Neuron* **42**, 983 (Jun 24, 2004).
2. P. Soriano, *Nat. Genet.* **21**, 70 (1999).
3. J. Z. Tsien, P. T. Huerta, S. Tonegawa, *Cell* **87**, 1327 (1996).
4. K. Nakazawa *et al.*, *Science* **297**, 211 (Jul 12, 2002).
5. T. Iwasato *et al.*, *Neuron* **19**, 1201 (1997).
6. W. W. Anderson, G. L. Collingridge, *J Neurosci Methods* **108**, 71 (Jul 15, 2001).
7. M. S. Fanselow, *Pavlov J Biol Sci* **15**, 177 (1980).
8. T. J. McHugh, K. I. Blum, J. Z. Tsien, S. Tonegawa, M. A. Wilson, *Cell* **87**, 1339 (1996).
9. S. Leutgeb, J. K. Leutgeb, E. I. Moser, M. B. Moser, *Hippocampus* **16**, 765 (2006).
10. S. Leutgeb *et al.*, *Science* **309**, 619 (Jul 22, 2005).
11. S. Leutgeb, J. K. Leutgeb, A. Treves, M. B. Moser, E. I. Moser, *Science* **305**, 1295 (Aug 27, 2004).
12. B. A. Boston, K. M. Blaydon, J. Varnerin, R. D. Cone, *Science* **278**, 1641 (Nov 28, 1997).
13. B. M. King, *Physiol Behav* **87**, 221 (Feb 28, 2006).
14. R. G. Morris, P. Garrud, J. N. Rawlins, J. O'Keefe, *Nature* **297**, 681 (Jun 24, 1982).
15. K. D. Harris, D. A. Henze, J. Csicsvari, H. Hirase, G. Buzsaki, *J Neurophysiol* **84**, 401 (2000).